Supporting Information

Enhanced Stabilisation of Tetragonal (*t*) - ZrO_2 in the Controlled Nanotubular Geometry

Hyunchul Kim,[†,ǀ] *Myungjun Kim,* [†,ǀ] *Changdeuck Bae,*[†, ‡,*] *Eunsoo Kim,*[†] *Seonhee Lee,*[†] *Josep M. Montero-Moreno,*[§] *Hyun Suk Jung,*[#] *and Hyunjung Shin*[†,*]

[†]Department of Energy Science, Sungkyunkwan University, Suwon 440-746, South Korea

[‡]Integrated Energy Center for Fostering Global Creative Researcher (BK 21 plus), Sungkyunkwan University, Suwon 440-746, South Korea

[§]Institute of Applied Physics, University of Hamburg, Jungiusstrasse 11, 20355, Hamburg, Germany

[#]School of Advanced Materials Science and Engineering, Sungkyunkwan University, Suwon 440-746, South Korea

[*] To whom correspondence should be addressed. Electronic mails: changdeuck@skku.edu and hshin@skku.edu

[ǀ] H.K. and M.K. contributed equally to this work.

Table S1. Thermodynamic equations for nanocrystalline ZrO_2 with sphere- and disc-like grains.

Sphere	Disc
	
$G = 4/3\,\pi r^3\psi + 4\,\pi r^2\sigma + 4/3\,\pi r^3\varepsilon$	$G = \pi r^2 e\,\psi + (2\pi re + 2\pi r^2)\sigma + + \pi r^2 e\,\varepsilon$
$r_c = \dfrac{(-3)(\sigma_t - \sigma_m)}{q(1 - T/T_b) + (e_t - e_m)}$	$r_c = \dfrac{(-2)\,(\sigma_t - \sigma_m)}{\frac{2}{e}(\sigma_t - \sigma_m) + q(1 - T/T_b) + (e_t - e_m)}$

Sphere versus disc geometries

Energy of crystal with sphere-like grains can be descrived by three terms (after Shukla and Seal):

- Energy related to the volume of an infinite strain free single crystal:

$$4/3\pi r^3\,\psi$$

- Energy related to the surface of the crystal:

$$4\pi r^2\sigma$$

- Energy related to crystal strain (affects the total volume of the crystal:

$$4/3\pi r^3\varepsilon$$

Then, we get an equation

$$G = 4/3\pi r^3\psi + 4\,\pi r^2\sigma + 4/3\pi r^3\varepsilon$$

where G, total free energy of spherical crystal; r, radius of spherical crystal; ψ, volume free energy (J/m^3) of an infinite strain free single crystal; σ, surface free energy (J/m^2) of the spherical crystal.

$$\Delta G_{m\to t} = G_t - G_m$$

$\Delta G_{m\to t} < 0 \rightarrow t$ is the stable phase

$$\Delta G_{m\to t} > 0 \to m \text{ is the stable phase}$$

$$\Delta G_{m\to t} = 4/3\pi r^3(\psi_t - \psi_m) + 4\pi r^2(\sigma_t - \sigma_m) + 4/3\pi r^3 (\varepsilon_t - \varepsilon_m)$$

At the $m\to t$ transformation:

$$\Delta G_{m\to t} = 0,\ r\to r_c \text{ (critical radius)}$$

Therefore,

$$r_c = \frac{(-3)(\sigma_t - \sigma_m)}{(\psi_t - \psi_m) + (\varepsilon_t - \varepsilon_m)}$$

As for the disc-like grains:

- Energy related to the volume of an infinite strain free single crystal:

$$\pi r^2 e\,\psi$$

- Energy related to the surface of the crystal:

$$2\pi re + 2\pi r^2\sigma$$

- Energy related to crystal strain (affects the total volume of the crystal:

$$\pi r^2 e\,\varepsilon$$

Then,

$$G = \pi r^2 e\,\psi + (2\pi re + 2\pi r^2)\sigma + \pi r^2 e\,\varepsilon$$

$$\Delta G_{m\to t} = \pi r^2 e\,(\psi_t - \psi_m) + (2\pi re + 2\pi r^2)(\sigma_t - \sigma_m) + \pi r^2 e\,(\varepsilon_t - \varepsilon_m)$$

$$r_c = \frac{(-2)\,(\sigma_t - \sigma_m)}{\frac{2}{e}(\sigma_t - \sigma_m) + (\psi_t - \psi_m) + (e_t - e_m)}$$

Since for a bulk single crystal:

$\Delta\psi = (\psi_t - \psi_m) = q(1 - T/T_b)$

where q, latent heat of transformation (J·m^{-3}) for a bulk single crystal; T_b, *transition temperature for a bulk single crystal* (note that the bulk single crystal would be equivalent to the infinite strain free single crystal mentioned above).

Table S2. Experimental values collected after Shukla and Seal and used for the simulations.

q (bulk single crystal)	2.89×10^8 J/m^3
q (spherical nanocrystal)	1.21×10^8 J/m^3
$\sigma_t - \sigma_m$ (for isolated particle)	-0.36 J/m^3
$\sigma_t - \sigma_m$ (for aggregated particle)	-1.24 J/m^3
Non-hydrostatic strain energy	0 to -2.8×10^6 J/m^3
T_b	1448 K
e	11.5 nm

We consider the crystal as a bulk single crystal or apply the correction for nanocrystals, where q (latent heat of transformation) decreases (possibly the most realistic). It is assumed that latent heat of transformation (q) does not change with temperature. The crystal can be considered issolated in the matrix or in an aggregated condition. These affects the values of the interfacial energies, as reported by Garvie, and hence the $\sigma_t - \sigma_m$ difference.

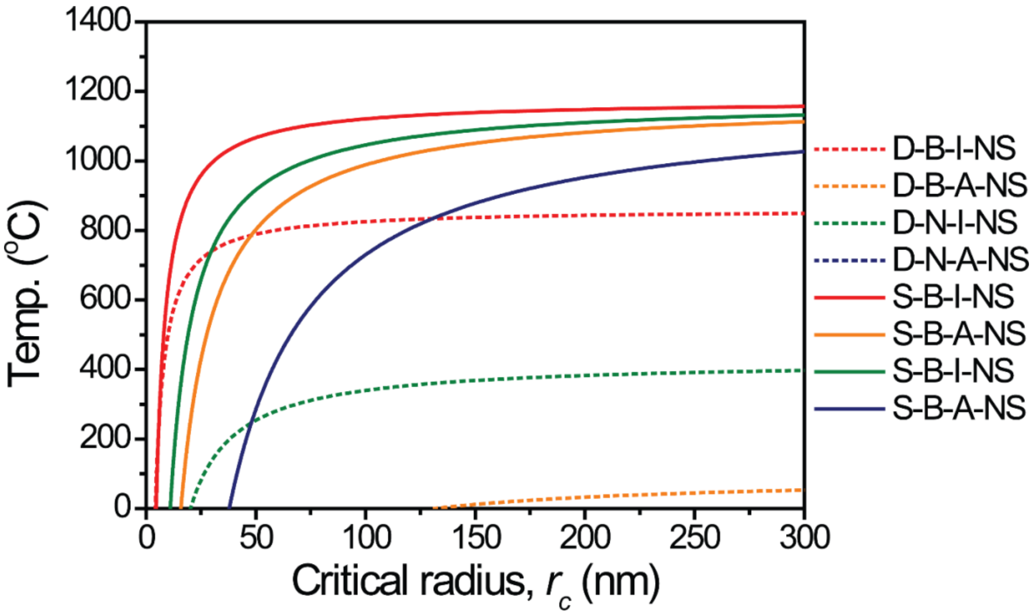

Figure S1. Comparison of spherical (solid lines) and disk (dash lines) geometries under different modification conditions.

Nomenclature description used in Fig.S1 is given below:

Spherical (**S**), $r_c = \frac{(-3)(\sigma_t - \sigma_m)}{q(1 - {}^{T}/{T_b}) + (e_t - e_m)}$

Disc (**D**), $r_c = \frac{(-2)\ (\sigma_t - \sigma_m)}{\frac{2}{e}(\sigma_t - \sigma_m) + q(1 - {}^{T}/{T_b})\ +\ (e_t - e_m)}$

Bulk (**B**), $q = 2.89 \times 10^8$ J/m³

Nanosized (**N**), $q = 1.21 \times 10^8$ J/m³

Isolated (**I**), $\sigma_t - \sigma_m = -0.36$ J/m²

Aggregated (**A**), $\sigma_t - \sigma_m = -1.24$ J/m²

Not strained (**NS**), $(e_t - e_m) = 0$ J/m³

Strained (non-hydrostatic, **SXX**), $(e_t - e_m) = 0.35$ to 2.80×10^8 J/m³

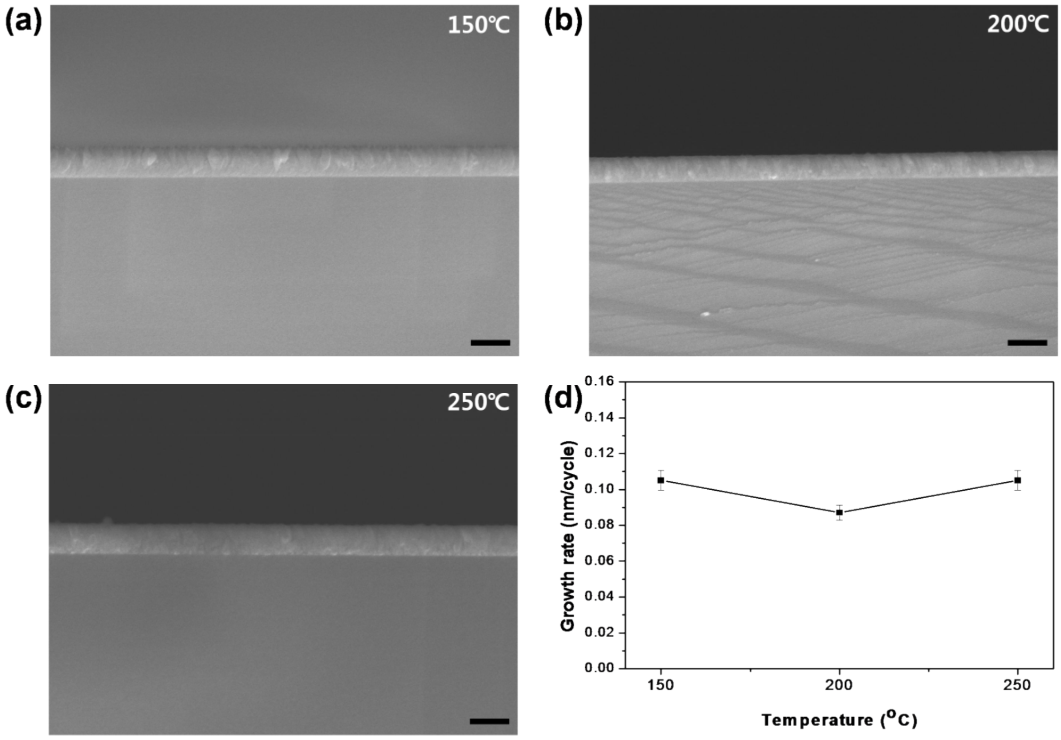

Figure S2. SEM images of ZrO_2 thin films were produced by 1500 ALD cycles onto Si (100) substrates at (a) 150, (b) 200, and (c) 250 ^{o}C. Both TEMAZr and D.I. water exposure times were 2s and Ar gas purge time was 8s. All scale bars on SEM images represents 100nm. (d) Growth rate of ZrO_2 films were 0.105±0.005 nm/cycle, 0.087±0.004 nm/cycle, and 0.105±0.006 nm/cycle at 150, 200, and 250 ^{o}C, respectively.

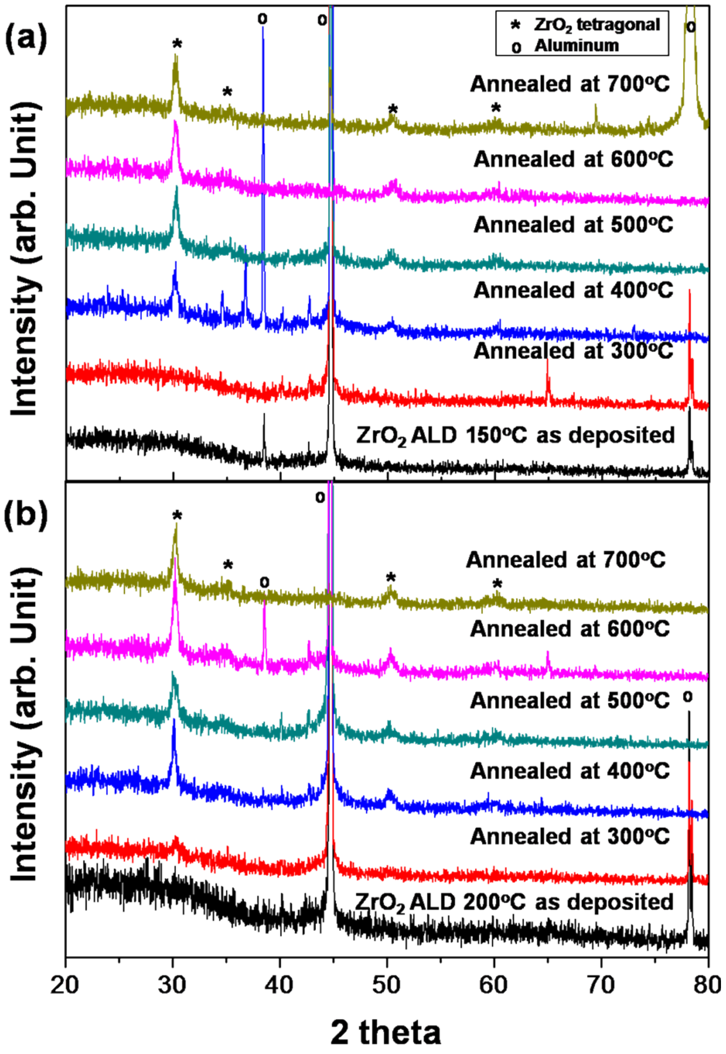

Figure S3. XRD patterns of ZrO_2 nanotubes as-grown at (a) 150 and (b) 200 °C, followed by annealing at different temperatures up to 700 °C.

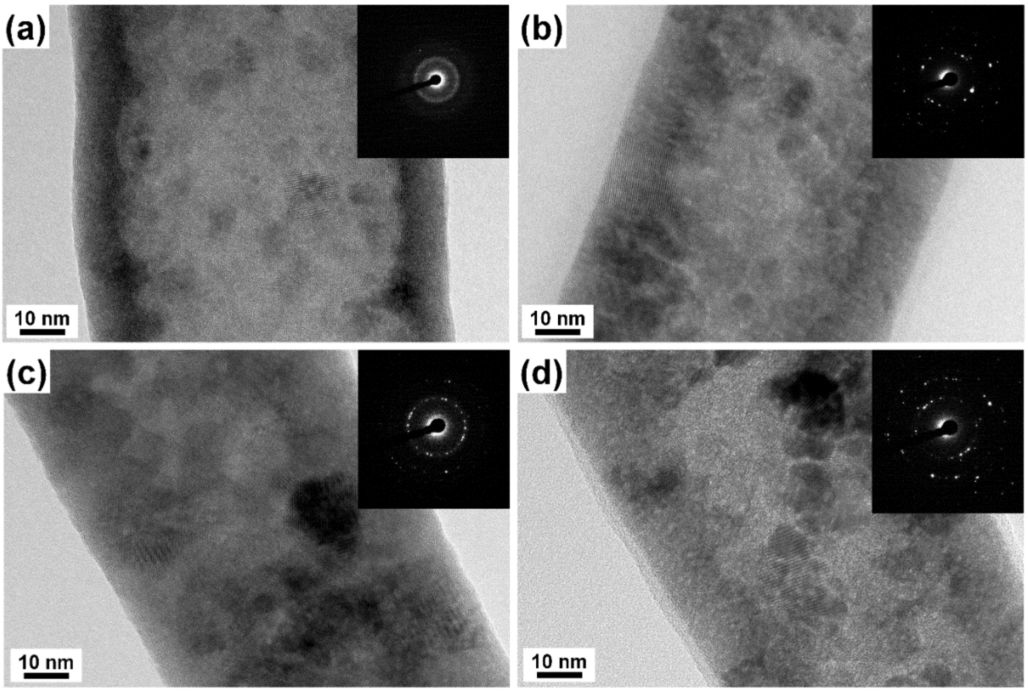

Figure S4. TEM observation of the post-annealed ZNTs at T_{sub} = 300 (a, c) and 400 °C (b, d) with samples at different as-deposition temperatures of T_{sub} = 150 °C (a-b) and 200 °C (c-d). The gradual increase in the resulting nanocrystalline grains is visible in bright field images and electron diffraction patterns, in proportional with T_{sub}.

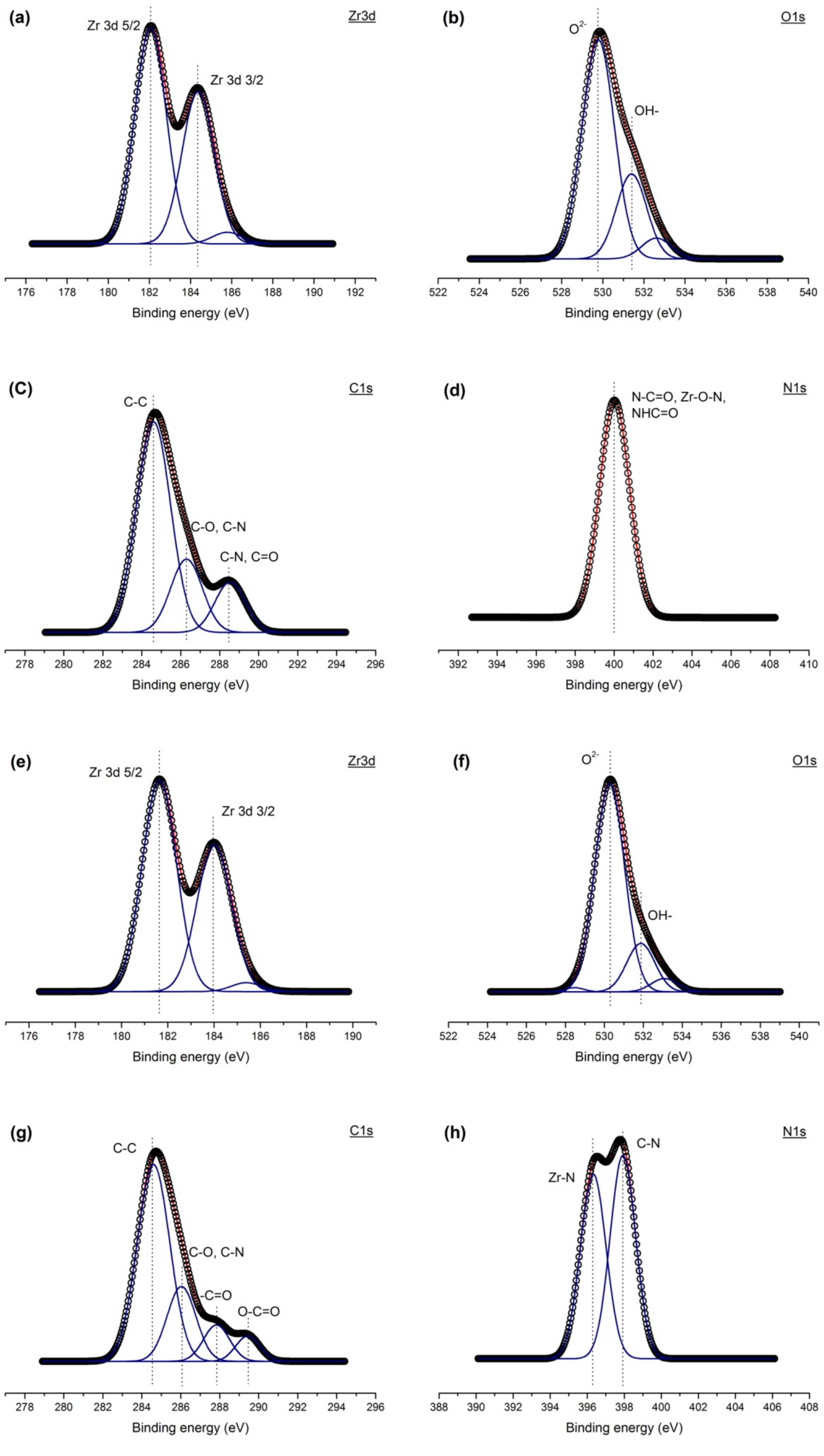
(a)
Zr3d
Zr 3d 5/2
Zr 3d 3/2
176 178 180 182 184 186 188 190 192
Binding energy (eV)
(b)
O1s
O^{2-}
OH-
522 524 526 528 530 532 534 536 538 540
Binding energy (eV)
(C)
C1s
C-C
C-O, C-N
C-N, C=O
278 280 282 284 286 288 290 292 294 296
Binding energy (eV)
(d)
N1s
N-C=O, Zr-O-N,
NHC=O
392 394 396 398 400 402 404 406 408 410
Binding energy (eV)
(e)
Zr3d
Zr 3d 5/2
Zr 3d 3/2
176 178 180 182 184 186 188 190
Binding energy (eV)
(f)
O1s
O^{2-}
OH-
522 524 526 528 530 532 534 536 538 540
Binding energy (eV)
(g)
C1s
C-C
C-O, C-N
-C=O
O-C=O
278 280 282 284 286 288 290 292 294 296
Binding energy (eV)
(h)
N1s
Zr-N
C-N
388 390 392 394 396 398 400 402 404 406 408
Binding energy (eV)

Figure S5. XPS investigation of ALD-grown ZrO_2 before (a-d) and after (e-h) annealing at 700 °C at 1 hr. C and N impurities were detected. Most probably, they came from the precursor molecules having amine moiety and even upon annealing treatments.

Table S3. A summary of grain sizes that were determined by TEM statistics and Scherrer equation.

As-deposited [TEM diameter]	150 ℃	200 ℃	250 ℃	
	4.3 ± 1.4 nm	6.8 ± 2.2 nm	15.1 ± 3.7 nm	
Annealed (700 ℃) [Scherrer diameter]	16.5 nm	17.5 nm	17.1 nm (T)	52.7 nm (M)

Scherrer Equation

$$L = \frac{K\lambda}{B\ cos\theta}$$

Where L is the crystallite size, K is a crystallite-shape factor (it varies from 0.62 to 2.08; here 0.9 was used assuming spherical crystals), λ is the wavelength of the X-rays (0.154 nm for Cu $K\alpha_1$), B is the width (full-width at half-maximum) of the X-ray diffraction peak in radians, and θ and the Bragg angle.